Astroparticle Physics 1 (1992) 61–76
North-Holland

Astroparticle Physics

A new investigation on neutralino dark matter: relic density and detection rates

A. Bottino, V. de Alfaro, N. Fornengo, G. Mignola and S. Scopel

Dipartimento di Fisica Teorica dell'Università di Torino, and INFN, Sezione di Torino, Via Giuria 1, 10125 Torino, Italy

Received 18 July 1992

The main properties of the neutralino dark matter are revisited in the light of the new theoretical developments in Su theories and of the recent constraints from accelerators and underground experiments. The neutralino relic abundance an the detection rates relevant for direct and indirect searches are evaluated in the minimal supersymmetric standard mod (MSSM) with the full inclusion of the (one-loop) radiative corrections, both to the Higgs masses and to the trilinear Hig self-coupling. The relevance of these corrections for the neutralino–neutralino annihilation cross-section, and thus for th relic density, is discussed in detail. Large regions of the parameter space are considered, including those where th neutralino only provides a fraction of the local dark matter density; in these domains the standard value for the local densi is appropriately scaled down. Some general properties of the detection rates as functions of the MSSM parameters are als elucidated; in particular it is shown that in the regions of the parameter space where scaling of the local density occurs, th rates are largely independent of two of the model free parameters. The relevance of the Kamiokande upper bounds to th upgoing muon fluxes is discussed in connection with the possible neutrino outputs from the Earth and from the Sun due t neutralino accumulation and annihilation in these macroscopic bodies. Finally, the complementarity between the search fc neutralino dark matter and the discovery potential of future accelerators is discussed.

1. Introduction

A common feature of almost any analysis of the distribution of structures at different scales is the need for cold dark matter (CDM) at least as a component of the total amount of DM, even though the detailed conclusions of the various analyses may show differences according to the models and methods employed. Indeed it is reasonable to think that DM is made of different components, according to the type of particles that compose it and to their interactions.

A most interesting indication that adds circumstantial support in this sense comes from the very recent data by the COBE satellite on the anisotropic effects in the temperature distribution of the cosmic microwave background radia tion [1]. Important clues about the composition o DM result from the analysis performed in ref. [2 in terms of dynamical models of structure forma tion. The data on the cosmic microwave back ground radiation have been compared with re sults of structure formation in models of open o flat universes containing various percentages o different components of DM: CDM, HDM baryons and possibly a vacuum energy contribu tion. In terms of the density parameter of th universe $\Omega = \rho/\rho_c$, where ρ_c ($= 1.88 \times 10^{-29} h^2$ cm^{-3}, $0.4 \leq h \leq 1$) is the critical density, we writ

$$\Omega = \Omega_B + \Omega_{CDM} + \Omega_{HDM} + \Omega_{vac}. \qquad (1.1$$

Even though the models examined in ref. [2 belong to very different categories, the followin main conclusions may be drawn: DM is very likel to be a multicomponent system; CDM is presen

Correspondence to: A. Bottino, Dipartimento di Fisica Teorica dell'Università di Torino, Via Giuria 1, 10125 Torino, Italy.

in all models, and is thus a necessary ingredient (together of course with an amount of baryonic matter in agreement with nucleosynthesis).

One more remarkable feature emerges from the examples discussed in ref. [2], i.e. that, independently of the dynamical model of structure formation employed to fit the COBE data, the fractional contribution of CDM to the total relic density appears to be constrained into a rather narrow range

$$\Omega_{\mathrm{CDM}} h^2 = 0.1 - 0.2. \tag{1.2}$$

It will be extremely interesting to see whether this feature will be confirmed by further analysis of the data and by independent observational results.

From the study of the spiral arms of galaxies a somewhat smaller determination of Ωh^2 is suggested. Indeed, if $\Omega_{\mathrm{gal}} \approx 0.1$, with a central value for $h^2 \approx 0.5$, one gets $\Omega h^2 \approx 0.05$. This value for Ω is believed to correspond to the local density $\rho_l \approx 0.3$ GeV cm^{-3} (see later the discussion about rescaling of the neutralino local density).

Since the neutralino (assumed here to be the lightest supersymmetric particle and denoted by χ) is a favourite candidate for CDM, a first question that we wish to address in the present paper is whether its relic abundance $\Omega_\chi h^2$ may be at the level of the present observational data or at least at a level which gives chances to direct and/or indirect searches for neutralino DM to be successful.

Neutralino as a candidate for CDM has already been considered in previous works [3–7] where $\Omega_\chi h^2$ has been evaluated under various assumptions. Here we present a new analysis where particular care is paid to the inclusion of the radiative corrections (RC), recently proved to be relevant to the phenomenology described by the minimal Susy standard model (MSSM) [8,9]. The radiative effects considered here go beyond those related to the Higgs masses and already included in previous works [3,6]; in fact, here, also corrections to coupling constants are included. In the present paper it is shown in particular that the interplay of the RC of different origins may cause sizeable cancellations in the amplitudes of some important neutralino–neutralino annihilation channels.

It is also shown that, in large regions of the MSSM parameter space, predictions for direct and indirect event rates are very insensitive to the variations of some of the free parameters of the Susy model. The other main points discussed in this paper concern the perspectives for neutralino DM searches and the complementarity between the discovery potential of these experiments and the information that can be obtained at the future accelerators. In this paper we consider neutralinos whose mass, m_χ, is comprised in a range which is above the present experimental lower bound [10,11] and within the reach of next accelerators, i.e. 20 GeV $\lesssim m_\chi \lesssim M_{\mathrm{W}}$.

2. Theoretical framework

The theoretical scenario considered here is the one provided by the MSSM, implemented by GUT conditions. The neutralino is defined to be the lowest-mass linear combination of photino, zino and higgsinos,

$$\chi = a_1\tilde{\gamma} + a_2\tilde{Z} + a_3\tilde{H}_1^0 + a_4\tilde{H}_2^0. \tag{2.1}$$

χ is assumed to be the lightest supersymmetric particle (LSP) and to be stable (by assuming R-parity conservation; for the case of R-parity violation see ref. [7,12]). Here, as usual, $\tilde{\gamma}$ and $\tilde{Z}$ are defined in terms of the U(1) gaugino and of the SU(2) neutral one by

$$\begin{aligned} \tilde{\gamma} &= \cos\theta_{\mathrm{W}}\,\tilde{B} + \sin\theta_{\mathrm{W}}\,\tilde{W}_3, \\ \tilde{Z} &= -\sin\theta_{\mathrm{W}}\,\tilde{B} + \cos\theta_{\mathrm{W}}\,\tilde{W}_3, \end{aligned} \tag{2.2}$$

where θ_{W} is the Weinberg angle.

The typical Higgs sector of the MSSM has two Higgs doublets which generate, by spontaneous symmetry breaking, two vev's: v_1 and v_2; these provide masses to the down-type quarks and to the up-type quarks, respectively. In the χ mass sector the MSSM contains a few free parameters: M_1 and M_2, which are the mass parameters of $\tilde{B}$ and $\tilde{W}_3$, respectively, the Higgs mixing mass pa-

rameter μ and $\tan\beta = v_2/v_1$. Embedding the MSSM in GUT provides the usual condition $M_1 = \frac{5}{3} M_2 \tan^2\theta_W$. Further mass parameters appear in the theory in connection with the MSS Higgs sector which contains three physical ne tral particles: two CP-even states h and H, o

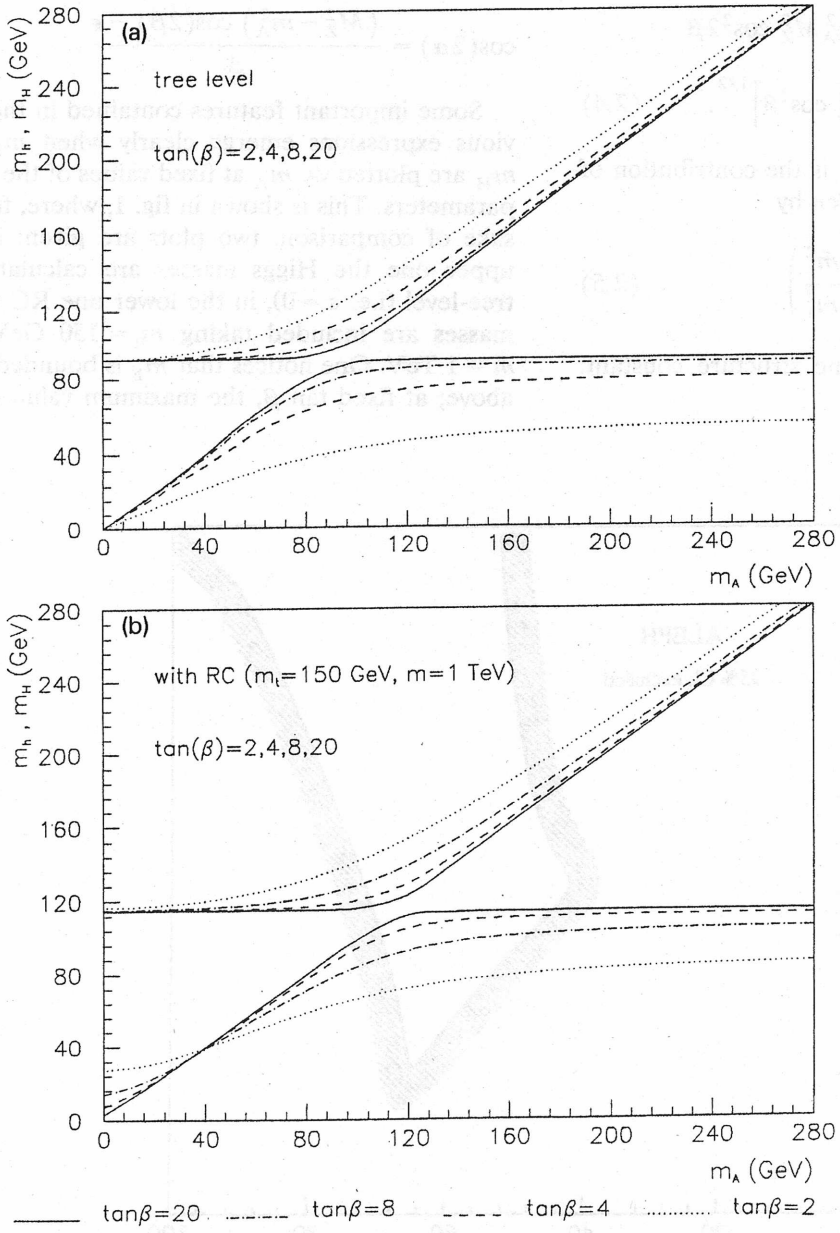

Fig. 1. Masses of the two scalar Higgs particles h and H as functions of the mass of the pseudoscalar Higgs A in the MSSM fc values of $\tan\beta = 2, 4, 8, 20$. (a) Tree-level results (i.e. $\epsilon = 0$). (b) RC to the masses are included. For the computation of RC, w have taken $m_t = 150$ GeV and $\tilde{m} = 1$ TeV.

CP-odd state A. Relationships among Higgs masses may be established [8,9]

$$m^2_{h,H} = \tfrac{1}{2}\left(m^2_A + M^2_Z + \epsilon \pm \Delta\right), \tag{2.3}$$

where

$$\Delta = \left[\left(m^2_A + M^2_Z + \epsilon\right)^2 - 4m^2_A M^2_Z \cos^2 2\beta - 4\epsilon m^2_A \sin^2\beta - 4\epsilon M^2_Z \cos^2\beta\right]^{1/2}. \tag{2.4}$$

In the two last equations ϵ is the contribution of the one-loop RC and is given by

$$\epsilon = \frac{3\alpha_W m^4_t}{2\pi M^2_W \sin^2\beta} \log\left(1 + \frac{\tilde{m}^2}{m^2_t}\right), \tag{2.5}$$

where α_W is the SU(2) fine structure constant: $\alpha_W = g^2/4\pi$.

This introduces in the neutral Higgs mass relations a dependence on the top quark mass m_t and on the degenerate mass $\tilde{m}$ of its scalar Susy partners. The mixing angle α, related to the diagonalization of the mass matrix for the two CP-even neutral Higgs scalars, is given by

$$\cos(2\alpha) = \frac{\left(M^2_Z - m^2_A\right)\cos(2\beta) - \epsilon}{\Delta}. \tag{2.6}$$

Some important features contained in the previous expressions emerge clearly when m_h and m_H are plotted vs. m_A at fixed values of the other parameters. This is shown in fig. 1, where, for the sake of comparison, two plots are given: in the upper one the Higgs masses are calculated at tree-level (i.e. $\epsilon = 0$), in the lower one RC to the masses are included taking $m_t = 150$ GeV and $\tilde{m} = 1$ TeV. One notices that m_h is bounded from above; at fixed tan β, the maximum value of m_h

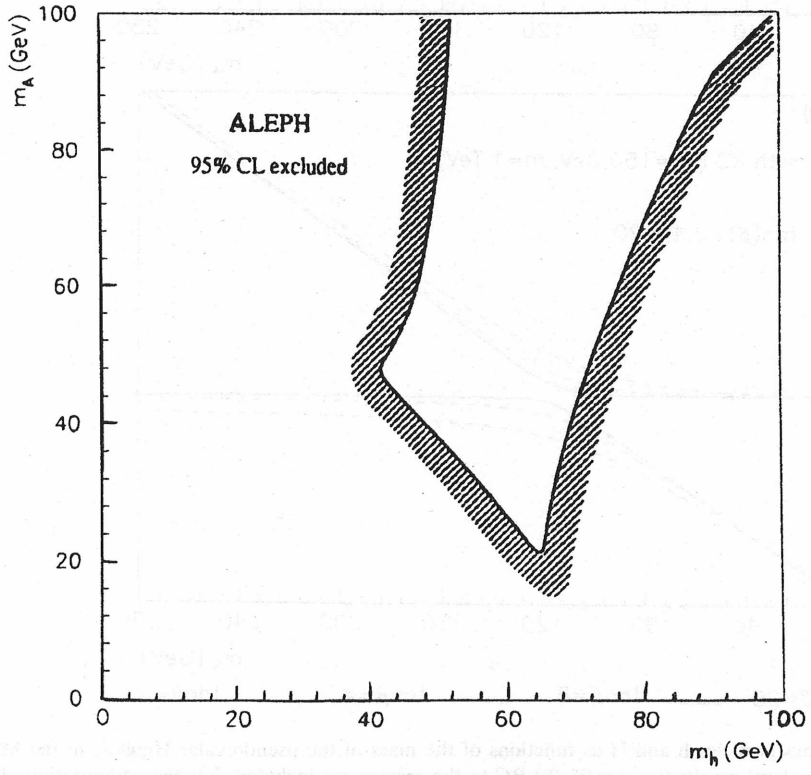

Fig. 2. Experimental bounds on m_h and m_A provided by the ALEPH collaboration at LEP (taken from ref. [13]).

is obtained for $m_A \to \infty$, and m_h reaches values very close to its maximum already at $m_A \approx 170$–200 GeV. Another interesting feature, which occurs only when RC are included, is represented by the possibility that h and A are both light and of the same order ~ 50 GeV, independently of the value for tan β.

Experimental bounds provided by accelerators about the MSSM Higgs sector are shown in fig. 2 in an m_h–m_A exclusion plot from the ALEPH collaboration at LEP [13].

Taking into account the relationships between the Higgs masses and the existing experimental constraints we select in the present paper a few representative points which correspond to different interesting scenarios: h and A both light, just above the experimental lower bounds, $m_h \approx m_A \approx 50$–60 GeV (tan $\beta = 8$ is taken for definiteness); h somewhat heavier, $m_h \approx 80$ GeV, with an A boson either of about the same mass (tan $\beta = 8$) or with a mass in the asymptotic regime, $m_A \approx 170$–200 GeV (tan $\beta = 2$).

In order to establish an appropriate range for M_2 we remind that in the hypothesis of equality of electroweak gaugino and gluino masses at GUT scale, one has $M_2 = m_{\tilde{g}}\alpha_2/\alpha_3 \simeq 0.3 m_{\tilde{g}}$, where m is the gluino mass. From this relation it follo that M_2 is of order of hundreds of GeV, if v assume that the gluino mass is $\lesssim 1$ TeV (Su ought to give at most this sort of scale, or it wou miss the main reason for its existence; furthe the present experimental limit from CDF [1 with the injection of some theoretical hypothes is $m_{\tilde{g}} \gtrsim 150$ GeV). For definiteness we consid here the range $0 \le M_2 \le 600$ GeV. According for μ we take the range -300 GeV $\le \mu \le 3($ GeV, which guarantees a parameter space wi enough to contain the different compositio (gaugino or higgsino like) for χ in the m_χ ran investigated here.

As for the values of the other masses, in wh follows we will use the representative values m = 150 GeV and $\tilde{m} = 1$ TeV.

3. The relic density

Let us turn now to the calculation of th neutralino relic density $\Omega_\chi h^2$. At variance wit previous evaluations we include here RC not on

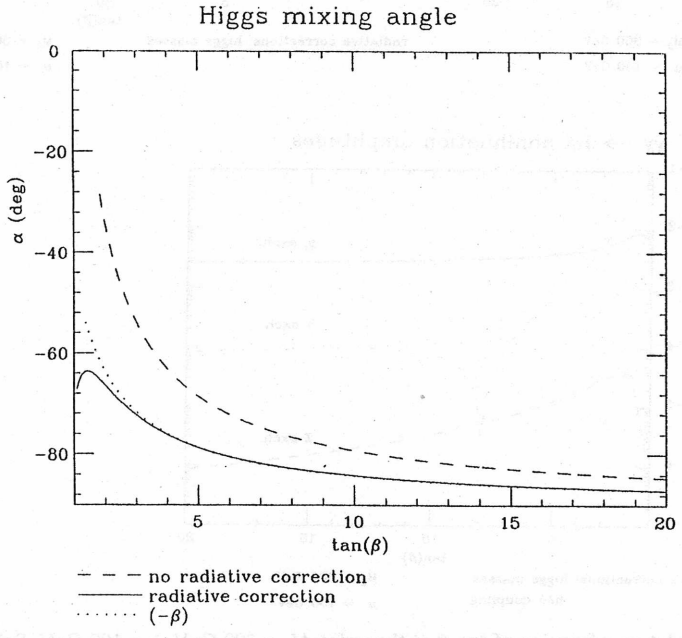

Fig. 3. Mixing angle α of the Higgs sector as a function of tan β. Dashed line: no RC; solid line: RC are included. The dotted lin represents the function $-\beta$. It is seen that, in the RC case, $\alpha \simeq -\beta$ for tan $\beta \gtrsim 2$–3 ($\alpha + \beta = 0$ occurs at about tan $\beta = 5$).

to the Higgs masses, but also to the trilinear Higgs self-coupling. The starting point is the standard formula [15]

$$\Omega h^2 = 2.13 \times 10^{-11} \left(\frac{T_\chi}{T_\gamma}\right)^3 \left(\frac{T_\gamma}{2.7\ \mathrm{K}}\right)^3 \times N_F^{1/2} \left(\frac{\mathrm{GeV}^{-2}}{a x_f + \frac{1}{2} b x_f^2}\right), \qquad (3.1)$$

where $x_f = T_f/m_\chi \simeq 1/20$ (T_f is the temperature at which the neutralino decoupled from the thermic bath), T_γ is the present temperature of the microwave background, T_χ/T_γ is the reheating factor for the photon temperature as compared to the neutralino temperature, N_f is the effective number of relativistic degrees of freedom at T_f. The quantities a and b which appear in the denominator of eq. (3.1) are the parameters entering in the non-relativistic expansion for the product of the pair-annihilation cross-section times the relative velocity thermally averaged at

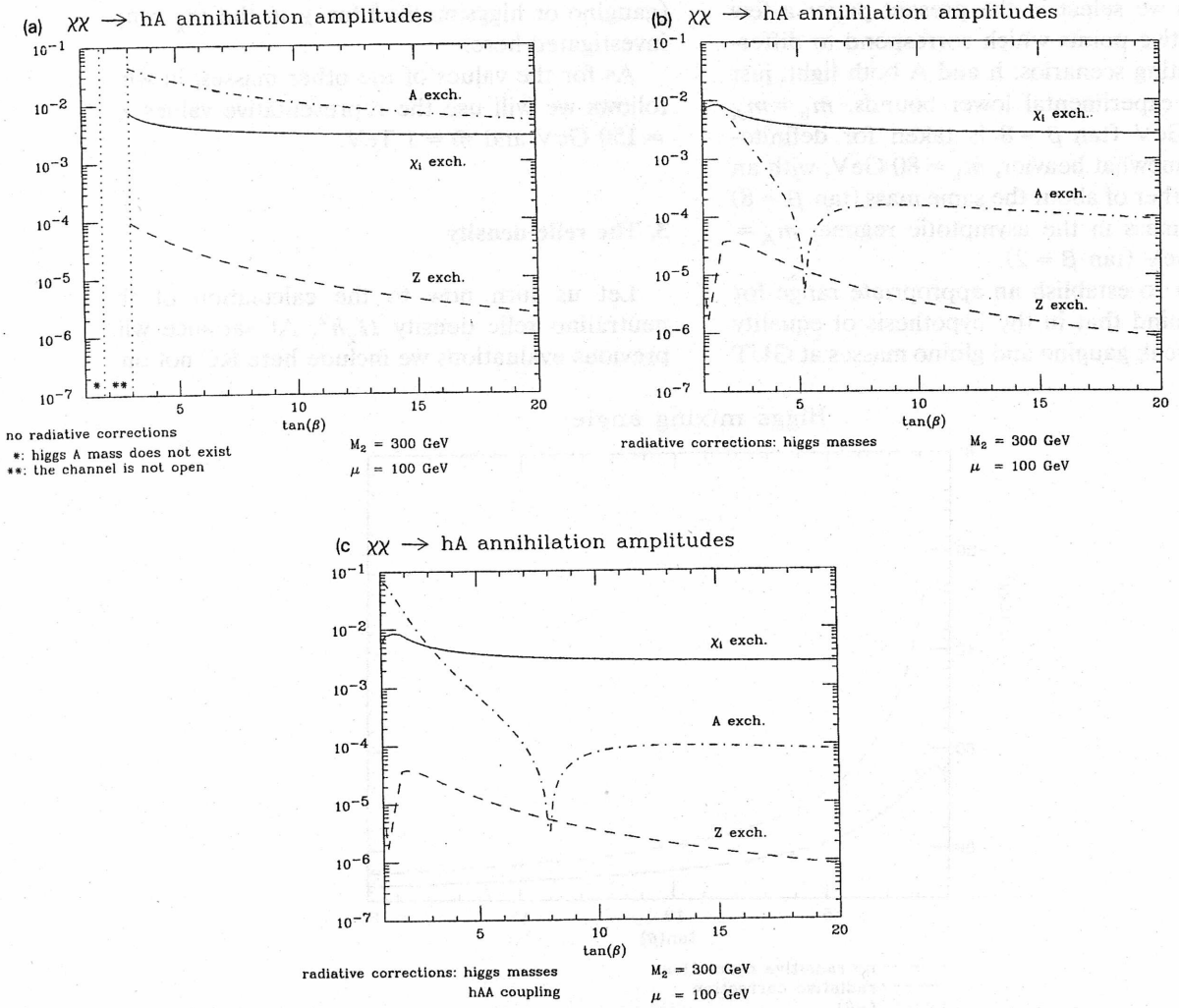

Fig. 4. Amplitudes for annihilation $\chi\chi \to$ hA as a function of tan β at the point $M_2 = 300$ GeV, $\mu = 100$ GeV. Solid line: amplitude due to exchange of intermediate χ_i's; dashed line: amplitude due to Z-exchange; dot-dashed line: amplitude due to A-exchange. (a) RC are not included; (b) RC to the Higgs masses are included; (c) also the RC to the coupling g_{hAA} have been included.

the temperature $T = xm_\chi$:

$$\langle \sigma_{\rm ann} v \rangle = a + bx. \qquad (3.2)$$

The expression $\langle \sigma_{\rm ann} v \rangle_{\rm int} \equiv a x_{\rm f} + \frac{1}{2} b x_{\rm f}^2$ appearing in (3.1) is due to the evolution in temperature from $T_{\rm f}$ to present.

The amplitudes which dominate in the χ–χ annihilation are those with a fermion–antifermion pair, f–$\bar{\rm f}$, or a pair of neutral Higgs in the final state. In the first case the three relevant diagrams are: Higgs-exchange diagram and Z-exchange diagram in the direct channel, $\tilde{\rm f}$-exchange diagram in the t channel. As far as the Higgs-exchange diagram is concerned, except when the A mass is large, say, $m_{\rm A} > 100$ GeV, annihilation through A is largely favoured, since at threshold the state $\chi\chi$ is pseudoscalar; for the h exchange the a term in eq. (3.2) is missing. For the $\tilde{\rm f}$-exchange diagram we notice that $\tilde{\rm q}$ exchange is strongly suppressed because of the experimental lower bound $m_{\tilde{\rm q}} \geq 150$ GeV [14]; in the slepton-exchange diagram we have taken $m_{\tilde{\rm l}} = 80$ GeV. In the case of two neutral Higgs bosons in the final state one still has contributions from Higgs exchange and from Z^0 exchange in the direct channel, whereas in the t channel exchange of the four neutralinos takes place. At the tree level, the exchange of the A boson to produce a pair hA in the final state is dominant. Inclusion of RC mo fies the situation strongly; it is here that RC different origins give rise to some subtle int play.

To see this,let us first consider the influence the radiative corrections to the Higgs masses the value of the mixing angle α. In fig. 3 we s that the inclusion of RC drastically changes t numerical relationship between α and β over wide range of tan β, making $\alpha + \beta$ almost vanis ing except for tan $\beta \lesssim 2$–3. This implies that t tree-level hAA coupling constant given by

$$\lambda_{\rm hAA} = \lambda^0_{\rm hAA} = -\frac{{\rm i}gM_{\rm Z}}{2\cos\theta_{\rm W}} \cos 2\beta \sin(\alpha + \beta) \qquad (3.$$

is drastically suppressed. This effect is manife by comparing fig. 4a with fig. 4b (the amplitud reported in these figures have been evaluated the arbitrary point $M_2 = 300$ GeV, $\mu = 100$ Ge for illustration). Inclusion of the one-loop RC the hAA coupling constant, under some simplif ing assumptions, modifies $\lambda_{\rm hAA}$ into [9]

$$\lambda_{\rm hAA} = \lambda^0_{\rm hAA} + \Delta\lambda_{\rm hAA}, \qquad (3.$$

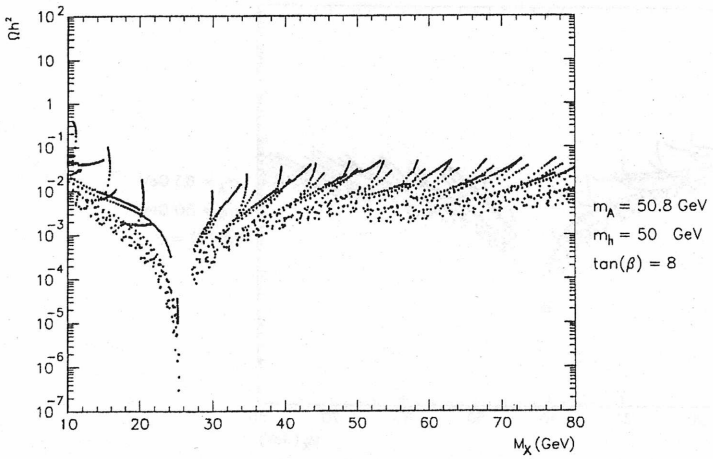

Fig. 5. $\Omega_\chi h^2$ as a function of the neutralino mass m_χ for tan $\beta = 8$, $m_{\rm h} = 50$ GeV, $m_{\rm A} = 50.8$ GeV.

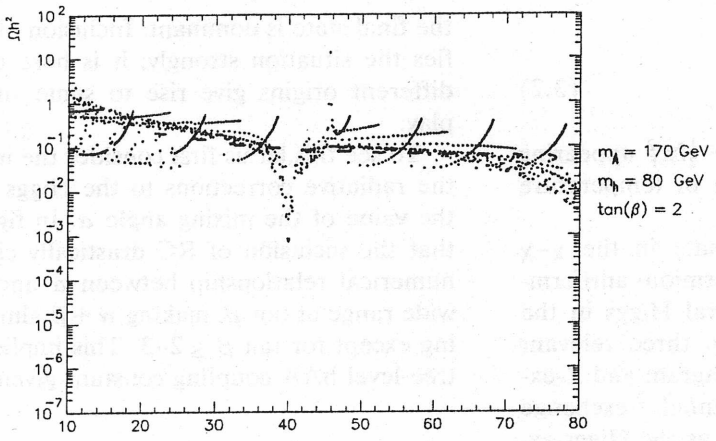

Fig. 6. $\Omega_\chi h^2$ as a function of the neutralino mass m_χ for $\tan\beta = 2$, $m_h = 80$ GeV, $m_A = 170$ GeV.

with

$$\Delta\lambda_{hAA} = \frac{-ig}{2M_W}\frac{\cos\alpha\cos\beta}{\tan\beta}\epsilon. \qquad (3.5)$$

This has the result of enhancing the A-exchange amplitude at small values of $\tan\beta$, as is shown in fig. 4c.

It is worth noticing that RC to other vertices (Z–Higgs–Higgs and $Z\bar{f}f$) are smaller (of order $\alpha_W m_t^2/M_W^2$) than RC to the trilinear Higgs vertex; thus they are neglected here.

In figs. 5–7 we show the values of $\Omega_\chi h^2$ at the representative points mentioned above. The spread of the data at any given value of m_χ is due to the span of parameters M_2, μ that correspond to that value of m_χ.

The general features of $\Omega_\chi h^2$ as a function of m_χ reflect the previous considerations. For small m_χ the annihilation goes into $f\bar{f}$, and $\Omega_\chi h^2$ decreases slowly up to the pronounced dip in correspondence to $m_\chi = \frac{1}{2}m_A$ due to the intermediate A in the direct channel; a smaller dip appears at $m_\chi = \frac{1}{2}m_h$, as is the case in fig. 6. The opening of the channel $\chi\chi \to hA$ is barely noticeable (see fig.

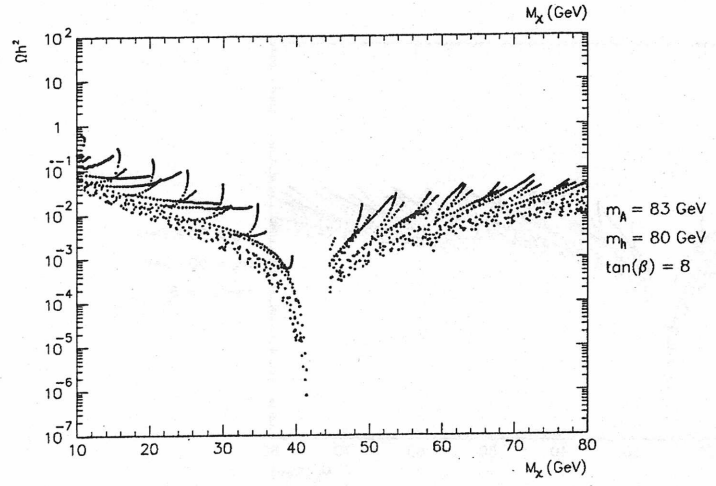

Fig. 7. $\Omega_\chi h^2$ as a function of the neutralino mass m_χ for $\tan\beta = 8$, $m_h = 80$ GeV, $m_A = 83$ GeV.